

Comparison of Velocity Shear with Turbulence Reduction Driven by Biasing in a Simple Cylindrical Slab Plasma

This article has been downloaded from IOPscience. Please scroll down to see the full text article.

2010 Plasma Sci. Technol. 12 391

(<http://iopscience.iop.org/1009-0630/12/4/02>)

View [the table of contents for this issue](#), or go to the [journal homepage](#) for more

Download details:

IP Address: 128.83.179.32

The article was downloaded on 10/03/2011 at 19:56

Please note that [terms and conditions apply](#).

Comparison of Velocity Shear with Turbulence Reduction Driven by Biasing in a Simple Cylindrical Slab Plasma

K. W. GENTLE, K. LIAO, K. LEE, W. L. ROWAN

Institute of Fusion Studies, University of Texas at Austin, Austin, Texas 78712, USA

Abstract In an experimental realization of the sheared cylindrical slab, the level of plasma turbulence is strongly reduced by application of a sufficient bias potential difference in the radial direction. Density fluctuation levels $\Delta n_{\text{rms}}/n$ decrease by more than a factor of five. The ion flow velocity profile is measured spectroscopically from the Doppler shift of an argon ion line. Comparison of the shearing rates with the turbulent amplitudes as a function of bias show no relation between the shearing rate and turbulence reduction, contrary to expectations.

Keywords: turbulence suppression, shear stabilization, velocity shear, bias

PACS: 52.35.Ra, 52.55.Dy

1 Introduction

Since turbulent-driven transport is the dominant transport process in nearly all high-temperature plasmas, understanding and control of turbulence is of paramount importance. Beginning with discovery of the “H-mode”^[1], numerous transitions and bifurcations to states of reduced turbulence and transport have been found^[2]. These are of great intrinsic interest for informing the physics of the turbulence as well as of practical significance in obtaining reduced transport rates. A common process in many of these transitions is the development of sheared flows, as has been thoroughly reviewed^[3]. Although flow shear is generally destabilizing in three-dimensional fluid turbulence, in the two dimensions of strongly magnetized plasmas, it has a stabilizing effect by shearing apart the unstable structures. Shear flow stabilization is a general effect expected in nearly any magnetized plasma, including a wide variety of biased configurations in both open and closed field lines^[3]. Provided the shear flow is not itself unstable (Kelvin-Helmholz), stabilization requires only a two-dimensional system for which the turbulence is not advected out of the shear flow before it can be modified - it remains longer than the turbulence decorrelation time, and for which the shearing rate is greater than the turbulence decorrelation rate - strong enough to disrupt the turbulence.

Although this picture is supported by extensive circumstantial evidence^[3], definitive tests have proven difficult because the flow shear is not generally under direct experimental control. The equilibrium state, including flows, is generally a self-consistent solution of equations including the turbulence and transport processes. Only initial and final steady states as a function of a few global parameters can be observed in a confined plasma. The present experiment allows more

direct control of the processes driving the flow and also greatly weakens the link between the equilibrium and the turbulent transport rate. It provides a broad range of shear flows over which turbulence reduction can be measured. Section 2 describes the experiment, section 3 presents the results, and section 4 offers conclusions.

2 Experiment setup

The experimental device is a Helimak^[4]. The magnetic configuration is that of a cylindrical (R, ϕ, z) slab with a dominant toroidal (azimuthal) field and a weak vertical (z) component so that the field lines are helices on a surface of constant radius. The plasma is generated by microwave power at the electron cyclotron frequency and is thus similar in some respects to that of Torpex^[5]. The plasma parameters are similar although the physical dimensions and thus many dimensionless parameters are quite different, for example the plasma size compared with turbulence correlation lengths. A cross-section is shown in Fig. 1. The radii of the inner and outer walls are 0.6 m and 1.6 m. The height is 2 m. The central magnetic field is typically 0.1 T. With a filling pressure of 2 mPa of argon, the maximum density approaches 10^{17} m^{-3} at an electron temperature of 10 eV. Because of symmetry and long mean free paths along the field lines, plasma parameters depend primarily on radius - the cylindrical slab. The density and temperature peak at radii somewhat greater than the radius for electron cyclotron resonance for the applied microwave power of 6 kW at 2.4 GHz, launched from the high field side.

For all values of the control parameters - fill pressure, toroidal field, and pitch, the plasma exhibits a high level, $\Delta n/n \geq 30\%$, of broadband turbulence with complicated structure. The radial correlation length

is less than 0.1 m, comparable with the density scale length and small compared with the system size, but large compared with $\rho_s \sim 0.02$ m, the ion gyroradius evaluated at the electron temperature. Therefore observations at each radius can be considered local and independent of behavior more than 0.1 m away. The correlation length in the z direction is somewhat longer, ~ 0.1 m. This specific magnetic configuration has been simulated with a fluid code [6], and the fluid model gives a reasonable account of the turbulence [7] as an interchange mode driven by the gradients in unfavorable magnetic curvature. In the region of negative density gradient well beyond the radius of maximum density, the turbulence propagates in the z direction (analogous to the poloidal direction in a tokamak) at a velocity of about 1000 m/s for typical parameters in argon. The wavenumbers fall in the range $0.1 < k_z \rho_s < 1$. The parallel wavenumbers are much smaller, between drift-wave values and the zero of interchange modes. Experimentally, it is difficult to distinguish between drift and interchange modes; the predicted propagation velocities are similar. The parallel wavelengths exceed 50 m, comparable with the parallel correlation length. The configuration constitutes a two-dimensional magnetized plasma, and the turbulence is likewise two-dimensional, fully meeting the first requirement for flow shear stabilization.

A special feature of this device is the ability to apply bias and alter the radial electric fields. Bias is applied using a set of metal plates, numbered 1~4 in Fig. 1, at the top and the bottom. The plates lie in the R, Z plane; the magnetic field is nearly perpendicular to the plates. Each plate is electrically isolated and has more than 35 surface-mounted Langmuir probes facing the plasma. (Only a few are represented in Fig. 1.) Provided the pitch of the field lines is not too large, all field lines will intercept the plates before reaching the top or bottom vessel walls. For these experiments, the connection length from top to bottom was 50 m (similar to the parallel correlation length) and the pitch was 0.2 m/turn at $R = 1.1$ m. Two sets of plates as shown in Fig. 1 are installed, 180° apart toroidally, to intercept all the field lines for this pitch. Since the purpose is to control the potential of the plasma on a magnetic surface (fixed R), all plates spanning the same range of R – the same number in Fig. 1 – are connected together. For normal operation, all plates are connected to the vacuum vessel ground. For biased operation, the four plates labeled 2 are connected to a controlled bias voltage. Although this bears some resemblance to edge biasing experiments in tokamaks [8], this experiment is simpler, with its uniform open field line configuration. The tokamak edge has closed magnetic surfaces coupling turbulence and transport tightly to the equilibrium and a transport constraint of conducting the entire tokamak input power. Here, the local turbulence responds only to the local drive with no global constraint. The turbulence is not flux-driven. This experiment is unique in directly measuring the ion flow velocity (V_z)

of the predominant plasma ion as the Doppler shift of the argon ion in a pure argon plasma.

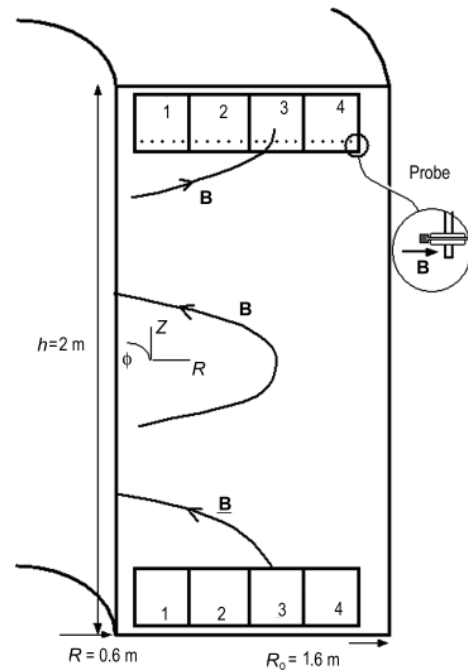


Fig.1 Schematic cross-section of the toroidal Helimak to scale, showing a helical field line and the plates at top and bottom on which the field lines terminate. The inset shows one of the several hundred probes mounted on the surface of the plates to measure equilibrium and fluctuating quantities (tip shaded)

3 Experimental results from biasing

Biasing drives a simple, strong bifurcation in the turbulence level, as illustrated in Fig. 2. The ion saturation current for a number of probes at different radii is shown as a function of time as the bias voltage on plate set 2 is swept from 0 V to -50 V and back to zero over the course of a twenty-second discharge. (The magnetic field and microwave power first reach their operating values at 7 s and are turned off at 27 s.) The turbulence level decreases, the average density may increase and $\Delta n/n$ decreases at the transition, with the quantitative results shown in subsequent figures. It is a bifurcation between two states with little modification as the threshold is approached from either direction. There is no hysteresis; the transition occurs at the same potential and current in each direction. The transition time, a few hundred milliseconds, is independent of the sweep rate of the bias voltage and is characterized by increasing quiet intervals between bursts of turbulence.

Common H-mode and internal transport barrier transitions are typically faster and sharper than those in the Helimak, even in a dimensionless measure, but this case is simpler because the drive is continuously and more directly controlled. The lack of hysteresis is an indication of this simplicity. In a well-confined

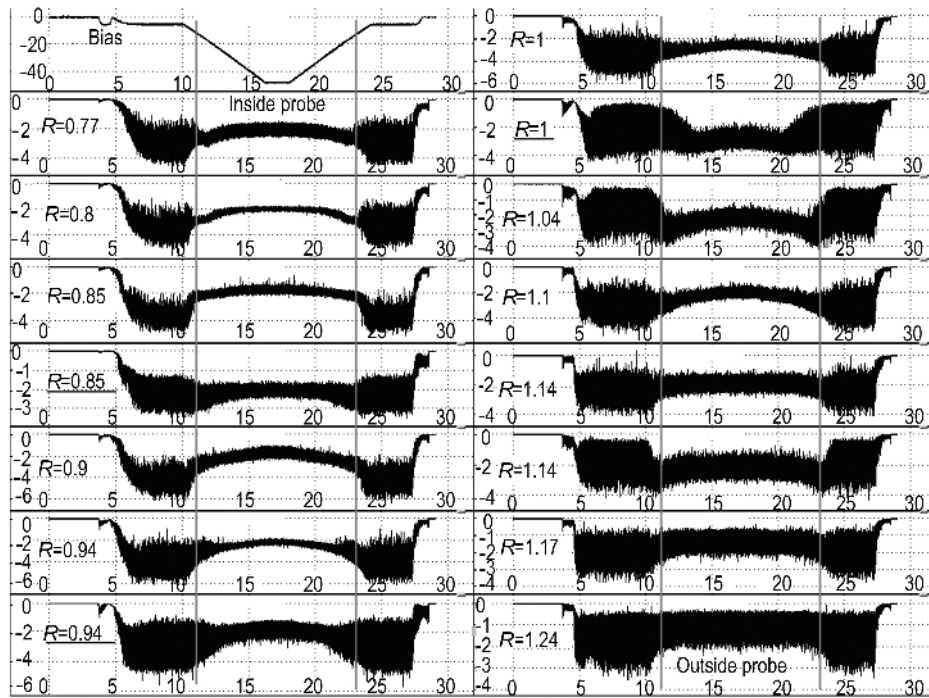


Fig.2 Ion saturation current (a.u.) to a selection of probes across the radius as the bias on plates 2 is swept to -50 V (top left panel), time from 0 s to 30 s. Underlined radii from probes on bottom plates. The transition (vertical lines) is symmetric, occurring at a voltage near -15 V

plasma like a tokamak, the change in transport during the transition quickly changes the plasma equilibrium state, speeding the transition and altering the requirements for the back transition. In the Helimak, flows to the top and bottom constitute a strong loss channel ($\sim 80\%$ of net particle loss) that is independent of radial turbulent transport. Quenching the turbulence makes only a modest change to the equilibrium state and does not alter the threshold condition.

Turbulence reductions are obtained for both negative and positive bias voltages. The radial profiles of density and floating potential for grounded plates and plates biased beyond the threshold are shown in Fig. 3. The density profiles show only modest changes. The electron temperatures (not shown) are nearly unchanged. The floating potentials generally move in the direction of biasing, but with attenuated magnitude. The plasma on the biased field lines does not simply float up with the bias voltage applied to the plates. Instead, the plates are conducting current, and the bias voltage appears largely as a sheath potential. The current, several amperes at the transition, flows radially through the plasma from the biased to the grounded plates. (The plates are connected through small shunt resistors to monitor the currents.) The turbulence levels ($\Delta n_{\text{rms}}/\langle n \rangle$) were measured for a set of bias voltages that span the range over which changes occur: $+10$ V, 0 V, 5 V, 10 V, -15 V, -20 V, and -25 V, as shown in Fig. 4. The positive case is the state of reduced turbulence for positive bias. At -10 V, the turbulence reduction is barely beginning. It is complete by -20 V; the turbulence levels for the -20 V and -25 V cases are indistinguishable.

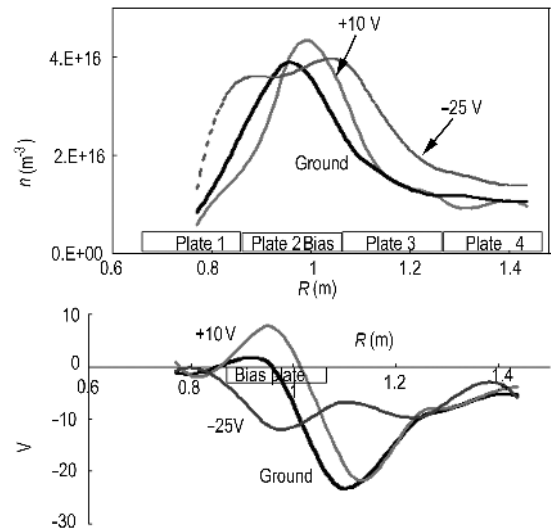


Fig.3 Equilibrium profiles with and without bias. (a) The density profiles are slightly modified, and (b) the floating potentials at the plate move in the direction of the applied bias

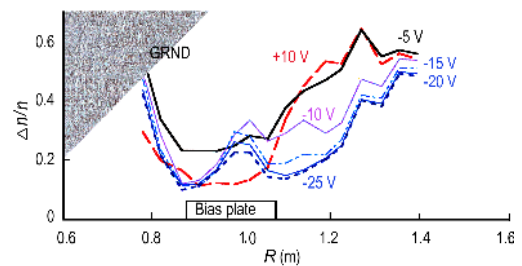


Fig.4 Profiles of the fractional level of density turbulence (rms) for various applied bias voltages

To assess the role of velocity shear in generating these turbulence reductions, the plasma flow transverse to the toroidal magnetic field was measured spectroscopically. The flow velocity was inferred from measurements of the Doppler shift of an argon ion line (Ar II 488.0 nm). The emission was viewed along a vertical chord with a 35 mm camera lens that images the plasma with a measured spatial resolution of 1 cm. The lens is fiber optically coupled to the entrance slit of a 1-m Czerny Turner spectrometer, the line is observed in 2nd order, and the diffracted image is detected with an intensified, linear CCD array. For a Gaussian line shape like that observed here, the uncertainty in determining the line center by least-squares fitting decreases with the square root of the spectral width and decreases directly with the signal-to-noise of the intensity [9] and can be much less than the line width or instrumental resolution. (The Gaussian shape observed here is largely of instrumental origin; intrinsic line width, Doppler ion thermal broadening, Doppler turbulent $\Delta \mathbf{E} \times \mathbf{B}$ broadening – roughly equivalent to a 1 eV temperature, and broadening caused by spatial variations over the viewing volume are all much smaller.) The signal was integrated over a few seconds during which plasma parameters and turbulence were stationary to increase the signal-to-noise of the intensity. Each individual spectral measurement was calibrated against a reference lamp to remove small variations in the measured wavelength that would otherwise have severely limited the measurement accuracy [10]. The uncertainty in velocity measurement was approximately 50 m/s, as shown in Fig. 5. This uncertainty corresponds to a shift of 0.0016 Å in second order and is consistent with older measurements [11] and modern instrumentation [12].

Since the singly ionized argon ion is the only ion species present and is cold, close to room temperature, the measured velocity is the mean fluid flow velocity. For cold ions, all drifts – the ion diamagnetic drift as well as the magnetic gradient and curvature drifts – are negligible; the flow is the $\mathbf{E} \times \mathbf{B}$ drift. Velocity profiles were obtained for the cases of Fig. 4. Velocity and velocity shear measurements are shown in Fig. 5. Velocity data points are shown for the grounded case; spline fits are shown for all cases. The base velocities are reasonable, less than 1000 m/s, the maximum electron diamagnetic velocity. The maximum implied electric field from $\mathbf{E} \times \mathbf{B}$ is less than 100 V/m. The integrated plasma potential variations across the profile are consistent with those inferred from the floating potential and temperature profiles, but this inference is subject to considerable uncertainty because it depends on the tail of the electron distribution function beyond $5T_e$. The changes induced by biasing are in the expected directions, but the plasma strongly modifies the radial profile of the effect.

The shear is calculated from the spline fits. A representative error estimate is shown for one point in Fig. 5(b) following TESTA et al. [13]. Since the stabilization mechanism depends only on the magnitude

of the shear and not its sign, only the magnitude is plotted. Local shearing rates can be quite large even in the unbiased case, as large as 5000 s^{-1} . In most theory and simulations, the criterion for shear stabilization is that the shearing rate exceed the linear growth rate. In experiments, the linear growth phase is never observed, only the nonlinearly saturated stationary state. However, the decorrelation rates can be determined from the measured autocorrelation functions. The decorrelation rate is both a quasi-linear estimate of the linear growth rate and a representation of the quantity that enters the general fluid theory, the eddy turnover rate [3].

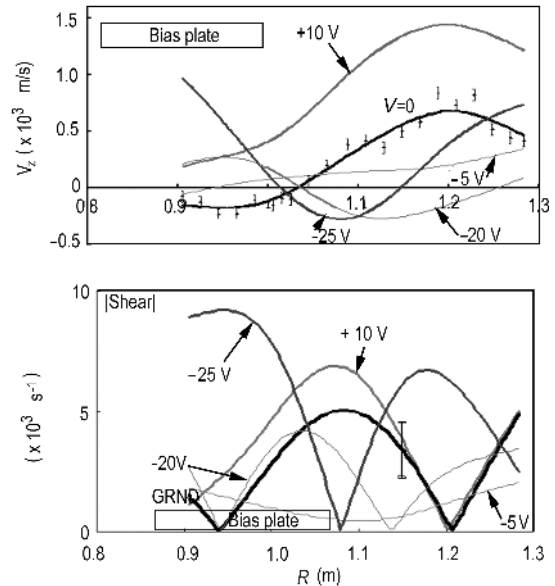


Fig.5 Profiles of (a) velocity and (b) the absolute magnitude of the velocity shear for various applied bias voltages. Measured velocity points shown for the grounded case. Spline fits shown for all cases. A representative error bar is shown for the shear inference. The sign of the shear is suppressed because the magnitude controls stability in the theory

The requirements for shear stabilization can be rephrased in terms of measured quantities. That the turbulence remain in the shear flow long enough to be affected, in this experiment, that the decorrelation rate must exceed the plasma loss rate, caused by the combined effects of parallel flow at the ion sound speed and measured V_z . These loss rates are less than 1000 s^{-1} , consistent with global estimates based on power input and total particle content. The loss rates are much less than the decorrelation rates, which exceed 2000 s^{-1} . The second, and usually critical, requirement is that the shearing rate exceed the decorrelation rate [3]. The experimental measurements are collected in Fig. 6. Each point represents an observation at one radius and one value of bias. The shearing rate is plotted against the reference decorrelation rate; the symbol indicates whether the turbulence level was normal (close to the value with no bias) or reduced for that radius. The diagonal dashed line separates the upper region, for which the shear is presumed to be sufficient to stabilize turbu-

lence, from the lower region, for which the shear is too weak. Although the slope of that line could arguably differ from unity, no choice would separate the normal from reduced turbulence points. All combinations occur: both normal and reduced turbulence levels occur at both high and low levels of relative shear.

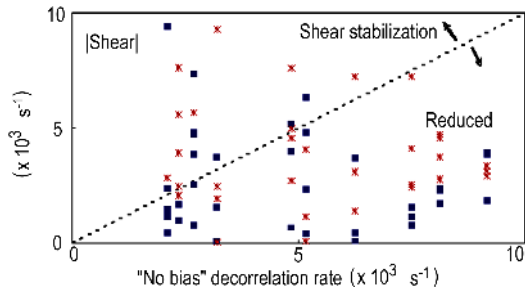


Fig.6 Velocity shearing rate vs. turbulence decorrelation rate for all radial positions and bias voltages. The dashed line represents the conventional criterion for shear stabilization

In this experiment, increased velocity shear does not explain the turbulence reduction. In addition to the results in Fig. 6, the data in Figs. 4 and 5 demonstrate that shear magnitudes are not uniformly increased for the cases with reduced turbulence. Biasing certainly modifies the velocity profiles and alters the shear pattern, but the shear is significantly larger only for -25 V, and only at some locations. However, the turbulence reductions are already complete at -20 V. Moreover, there are regions of strongly reduced turbulence where the shear remains low for values of the bias that cause the suppression.

The lack of correlation between turbulence amplitude and velocity shearing rate is summarized in Fig. 7, a scatter plot of shear magnitude vs. turbulent amplitude for all radii and all bias values. States of normal and reduced turbulence are distinguished, and a line to indicate the trajectory with changing bias from one typical radius is shown, a location for which turbulence is reduced only for negative bias. Although the application of bias can certainly reduce turbulence levels,

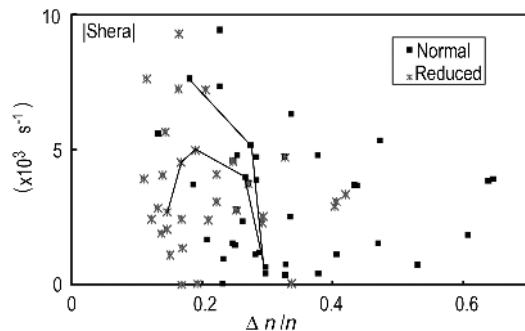


Fig.7 Velocity shear magnitude vs. density turbulence level. States with reduced turbulence levels compared with the no bias state indicated by stars. The points at $R = 1.06$ m are connected by a line to indicate a typical trajectory as a function of bias voltage

there is no indication that the mechanism involves flow shear. On the contrary, many of the instances of strongest turbulence reduction and lowest turbulence level occur at low flow shear, and the highest flow shear occurs with no turbulence reduction.

In addition to the density fluctuations, floating potential fluctuations and the turbulence-driven radial particle flux were also measured. Both are reduced by biasing in a manner qualitatively similar to density fluctuations, although the spatial profile of the reductions is slightly different for potential fluctuations. The turbulent flux is even more strongly reduced than the density-potential product, indicating that the phasing between density and electric field becomes less favorable for transport. Moreover, neither potential fluctuations nor transport reductions show any correlation with the velocity shear.

One aspect of the turbulence stabilization picture is supported by these experiments: turbulence reduction is associated with reduction in radial correlation length, the radial size of the turbulent structures. This is a fundamental and reassuring result, for the radial extent determines the quantity of gradient free energy available to drive the turbulence. This association is shown in Fig. 8. Although there is considerable scatter, the trend is correct and accounts for a significant fraction of the observed variation.

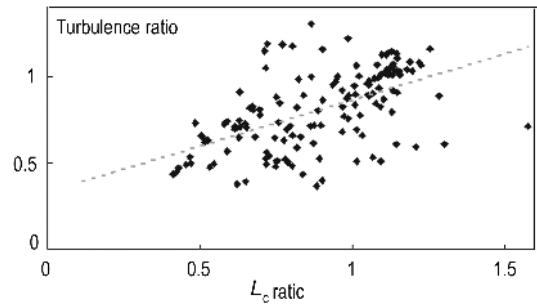


Fig.8 Relation between turbulence reduction and change in radial correlation length. The ratio of biased to unbiased turbulence level is plotted against the ratio of biased to unbiased radial correlation length. The dashed line is the best linear fit

4 Conclusions

The Helimak configuration provides an excellent, accessible example of saturated plasma turbulence driven by density and temperature gradients coupled to unfavorable magnetic curvature. The turbulence is generically similar to that in the outer region of a tokamak, and the Helimak may be modeled with the same codes as used for a tokamak scrape off layer. The configuration permits the controlled application of radial bias, sufficient values of which can significantly reduce the level of turbulence and transport. Although the bias does modify the flow velocity, there is no relation between the flow shear and the turbulence level or between the flow shear and the turbulence reduction, a

clear contradiction of theory under circumstances where the theory would be expected to apply. The conventional model should be re-examined. At the least, even if the standard model were not applicable to this instability for some reason, an additional mechanism to suppress turbulence must be found.

Acknowledgement

Work supported by the Department of Energy Office of Fusion Energy Sciences DE-FG02-04ER54766.

References

- 1 Wagner F, Becker G, Behringer K, et al. 1982 Phys. Rev. Lett., 49: 4208
- 2 Burrell K H. 1997, Phys. Plasmas, 4: 1499
- 3 Terry PW. 2000, Rev. Mod. Phys., 72: 109
- 4 Gentle K W, Huang H. 2008, Plasma Science and Technology, 10: 1
- 5 Müller S H, Fasoli A, Labit B, et al. 2004, Phys. Rev. Lett., 93: 165003
- 6 Ricci P, Rogers B N, Brunner S. 2008, Phys. Rev. Lett., 100: 225002
- 7 Li B, Rogers BN, Ricci P, et al. 2009, Phys. Plasmas, 16: 082510
- 8 Van Oost G, Adamek J, Antoni V, et al. 2003, Plasma Phys. Control. Fusion, 45: 621
- 9 Landman D A, Roussel-Dupre R, Tanigawa G. 1982, Astrophysical Journal, 261: 732
- 10 Meigs A G, Rowan W L, Woodward N W. 1990, Review of Scientific Instruments, 61: 2952
- 11 Meigs A G, Rowan W L. 1994, Physics of Plasmas, 1: 960
- 12 Rowan W L, Bespamyatnov I O, Granetz R S. 2008, Review of Scientific Instruments, 79: 10F529
- 13 Testa D, Garzotti L, Giroud C, et al. 2006, Nucl. Fusion, 46: 562

(Manuscript received 25 November 2009)

(Manuscript accepted 8 April 2010)

E-mail address of K. W. GENTLE:

k.gentle@mail.utexas.edu